



ELSEVIER

Contents lists available at ScienceDirect

Biosensors and Bioelectronics

journal homepage: www.elsevier.com/locate/bios

All electronic approach for high-throughput cell trapping and lysis with electrical impedance monitoring

Shideh Kabiri Ameri^a, Pramod K. Singh^a, Mehmet R. Dokmeci^{b,c,d}, Ali Khademhosseini^{b,c,d}, Qiaobing Xu^e, Sameer R. Sonkusale^{a,*}

^a Nano Lab, Department of Electrical and Computer Engineering, Tufts University, 161 College Avenue, Medford, MA 02155, USA

^b Center for Biomedical Engineering, Department of Medicine, Brigham and Women's Hospital, Harvard Medical School, Boston, MA 02115, USA

^c Harvard-MIT Division of Health Sciences and Technology, Massachusetts Institute of Technology, Cambridge, MA 02139, USA

^d Wyss Institute for Biologically Inspired Engineering at Harvard University, Boston, MA 02115, USA

^e Department of Biomedical Engineering, Tufts University, 4 Colby Street, Medford, MA 02155, USA

ARTICLE INFO

Article history:

Received 19 August 2013

Received in revised form

27 October 2013

Accepted 8 November 2013

Available online 18 November 2013

Keywords:

Dielectrophoresis

Cell trapping

Cell lysis

Microfluidics

High-throughput

ABSTRACT

We present a portable lab-on-chip device for high-throughput trapping and lysis of single cells with in-situ impedance monitoring in an all-electronic approach. The lab-on-chip device consists of microwell arrays between transparent conducting electrodes within a microfluidic channel to deliver and extract cells using alternating current (AC) dielectrophoresis. Cells are lysed with high efficiency using direct current (DC) electric fields between the electrodes. Results are presented for trapping and lysis of human red blood cells. Impedance spectroscopy is used to estimate the percentage of filled wells with cells and to monitor lysis. The results show impedance between electrodes decreases with increase in the percentage of filled wells with cells and drops to a minimum after lysis. Impedance monitoring provides a reasonably accurate measurement of cell trapping and lysis. Utilizing an all-electronic approach eliminates the need for bulky optical components and cameras for monitoring.

© 2013 Elsevier B.V. All rights reserved.

1. Introduction

Single cell analysis plays an important role in biological studies such as in the field of genomics, proteomics and metabolic engineering (Fritzsche et al., 2012; Marcy et al., 2007). Compared to the conventional approach of studying the culture of cells which measures average cell response, single cell studies allow one to catalog individual cell behavior and capture cellular heterogeneity. Techniques for isolating single cells in miniaturized platforms and studying them in a high-throughput manner are becoming essential in biological studies. There are various techniques for cell trapping such as using optical fields (Zhang and Liu, 2008), hydrodynamic forces (Valero et al., 2005), magnetic fields (Matthew et al., 2010), ultrasonic standing waves (Evander et al., 2007) and dielectrophoresis (DEP) (Kim et al., 2011). Among these methods, DEP-based cell trapping provides a low cost and efficient route to build such platforms for routine use in biology and medicine (Bocchi et al., 2009). This is because DEP is a fully electronic approach that does not require bulky and expensive optical components such as laser/light sources, objectives or lenses. DEP has the

potential to provide high-throughput parallel control of many individual cells. Furthermore, it is possible to trap different types of cells selectively and control them in both space and time. DEP has been used for various biological applications such as cell sorting (Cheng et al., 2009; Sano et al., 2011; Khoshmanesh et al., 2010) study of cell behavior and properties (J.E. Gordon et al., 2007; Morgan et al., 2007; Sun et al., 2007; Guido et al., 2012) and cell manipulation (Cha et al., 2011). In many biological investigations, after the cells have been captured through trapping, it is necessary to extract proteins or DNA from them for further downstream sensing and analysis. To perform such tasks, cell membrane must be ruptured to release cells organelles and other contents in a process that is termed lysis. Some popular approaches for cell lysis are through the use of chemical, mechanical and thermal means (Piersimoni et al., 2009; Baek et al., 2010; Di Carlo et al., 2003). Although these methods are simple, they are neither energy efficient nor do they have high yield. Moreover, they may not be appropriate for targeting specific cell types because they do not possess sufficient selectivity. Combining methods for selective trapping of specific cell types for lysis provide a robust platform for high quality cellular material extraction. Electrical approaches for cell lysis provides a highly controllable method, which can be combined with dielectrophoresis to provide an integrated low cost platform which is consistent with both high-throughput cell

* Corresponding author.

E-mail address: sameer@ece.tufts.edu (S.R. Sonkusale).

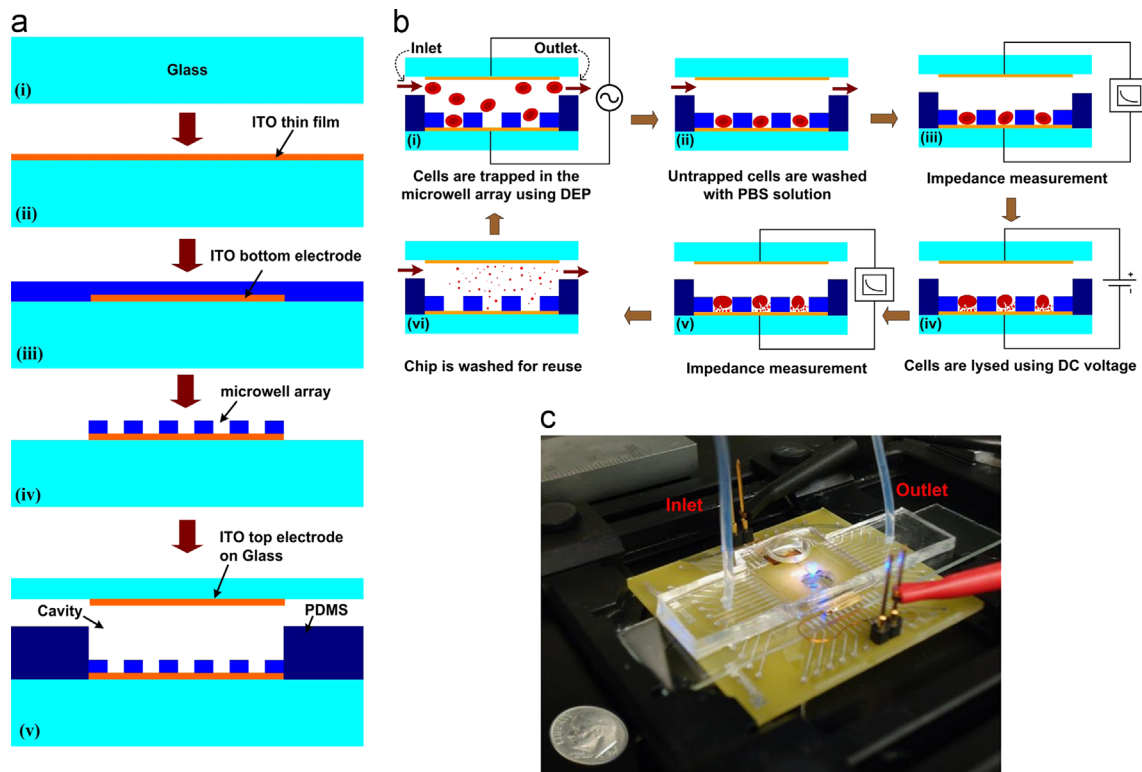


Fig. 1. (a) The fabrication process for the microfluidic HT cell trapping/lysis chip. (i) Start with a 3 in. glass substrate, (ii) coat with a thin film of ITO, (iii) create the bottom electrodes by patterning ITO film using photolithography and coat with SU8 (iv) fabricate SU8 based microwell array on top of the bottom electrode using photolithography, (v) create a PDMS microfluidic cavity with inlet and outlet channels; bound the top and bottom electrodes onto the PDMS microfluidic channels. (b) Experimental steps for cell trapping, lysis and impedance measurements. (c) Photo of the chip consisting of the microwell array, inlet, outlet and electronic connections; device placed next to a dime (10 cent) US coin.

trapping and lysis. There has been some work on combined trapping and lysis using electronic approaches (Kim et al., 2011; Jen et al., 2012; Sedgwick et al., 2008). However these platforms are still bulky and not amenable for lab-on-chip realization due to the need for optical or fluorescent microscopes for monitoring and characterizing DEP and lysis processes. For example, in a previous report (Kim et al., 2011), DEP is utilized with planar electrodes to trap single cells inside microwells with electrophoresis, and subsequently lyse them. Planar electrodes necessitate a physical approach for confinement to achieve effective lysing of cells. The whole process is monitored optically that still requires bulky optical instrumentation for characterization. Moreover none of the electronic method for combined trapping and lysis provides any precise control over the number of cells trapped in the microwells.

We have developed a high-throughput, non-optical approach for single cell trapping and lysis using electric fields, and in-situ monitoring based on impedance spectroscopy. The proposed platform consists of a single chip with 6400 microwells, sandwiched between two transparent electrodes with built-in microfluidic channels for cell delivery and extraction (Fig. 1(a)). An AC electric field is applied between the top and bottom electrodes to create a dielectrophoretic force for cell trapping. Then DC electric field is applied to lyse the cells. In this design, Indium Tin Oxide (ITO) has been used as the transparent conducting electrodes. Even though transparent electrodes were not necessary, their use will enable various optical imaging modalities (e.g. fluorescence). Impedance is measured both before and after trapping, and before and after lysis to measure the efficiency of cell trapping and lysis. This lab-on-chip platform allows for full electronic monitoring of cell trapping and lysis with an additional ability to perform optical monitoring.

2. Theory

The movement of a polarized dielectric particle as the result of a non-uniform electric field is known as dielectrophoresis (DEP) (Pohl, 1951). The DEP force, F_{DEP} , for a spherical particle with radius a , in the known electric field, E , can be calculated using the following relation (Kim et al., 2011).

$$F_{DEP} = 2\pi\epsilon_e a^3 \text{Re}[k(2\pi f)] |\nabla E|^2 \quad (1)$$

where ϵ_e is the permittivity of the external medium, f is the frequency and $k(2\pi f)$ is known as the Clausius–Mossotti and for the lossy dielectric is defined as

$$k(2\pi f) = \frac{\epsilon_{cell}^* - \epsilon_e^*}{\epsilon_{cell}^* + 2\epsilon_e^*} \quad (2)$$

the ϵ_e^* is the complex electrical permittivity of external medium and ϵ_{cell}^* is the electrical permittivity of the spherical particle and is defined as

$$\epsilon_{cell}^* = \epsilon_{cell} - j \frac{\sigma_{cell}}{2\pi f} \quad (3)$$

where σ_{cell} is the particle's conductivity. When the real part of Clausius–Mossotti factor is greater than zero, particles will move towards local maxima of the electric field, the process is known as positive dielectrophoresis. But when the real part of Clausius–Mossotti factor is smaller than zero, particles move towards minima of the electric field, and this process is known as the negative dielectrophoresis. Due to frequency dependent dielectric parameters, the Clausius–Mossotti factor, k , can be varied by changing the frequency of the applied field and by adjusting the

overall conductivity of the media. By changing the factor k , dielectrophoretic force can be adjusted from positive to negative or vice versa. Change from positive DEP to negative happens at a specific frequency known as the crossover frequency. The crossover frequency depends on the permittivity and conductivity of the particle and external medium, where both are a function of frequency. Cells can be manipulated using dielectrophoresis using this principle. However, cell membrane is double layer phospholipid which is more accurately modeled as a double-shell particle. Double-shell particle model for biological cell predicts presence of two crossover frequencies allowing one to adjust frequency to choose between positive and negative dielectrophoresis, for an attractive or repulsive force (Chung et al., 2011). Different cells have different permittivity and conductivity values and therefore their crossover frequencies are different, which may serve as a means of differentiating one cell type from another based on their response to AC dielectrophoresis (Gascoyne et al., 2009; Pommer et al., 2008). For instance Sano et al. (2011) reported a crossover frequency of 20 kHz for THP-1 human leukemia monocytes and 80 kHz for red blood cells. However even for the same type of cells crossover frequencies can change if the conductivity of the external medium changes (Hwang et al., 2008). Therefore background characterization of medium for its dielectric properties and conductivity is required to correctly estimate the crossover frequency for experimentation, which can be performed at the start of each use of the device for cell trapping and lysis.

3. Materials and methods

3.1. Device fabrication and experimental details

The fabrication process of microfluidic device for single cell trapping and lysis is shown in Fig. 1(a). ITO film with 200 nm thickness was deposited on a 3 in. glass substrate using DC magnetron sputtering (NSC 3000) which serves as transparent electrodes. The thickness of ITO thin film was measured by a surface profilometer (Veeco Dektak 6 M Stylus). Using standard lithography with positive photoresist (Rohm & Haas SPR220 series) and wet etching (HCl:H₂O:HNO₃=4:2:1), bottom and top electrodes were patterned. Electrodes were then annealed in nitrogen ambient at 300 °C for 1 h to improve their electrical

and optical properties. After annealing, the optical transparency of the ITO electrodes in the visible region increased considerably. The resistivity of ITO films was measured using a four point probe (Miller FPP-5000) and was found to be about $6.3 \times 10^{-3} \Omega \text{ cm}$. The negative photoresist (SU8 2005, MicroChem Co.) was then spin coated onto the bottom electrode to form a 7 μm thick layer. The SU8 photoresist was soft baked and exposed to UV light through photo-mask to form the microwells. After developing the photoresist, microwells that were 9 $\mu\text{m} \times 9 \mu\text{m}$ in area and 7 μm in depth were formed. The size of the wells was designed to be close to the diameter of the red blood cells to ensure that only a single cell would fit inside each well. To create the microfluidic channel and the cavity, first a SU8 master mold (100 μm in thickness) was prepared on a silicon wafer and then covered with a PDMS, base already was mixed with a curing agent in ratio at 10:1. The entire assembly then placed in a vacuum chamber to remove bubbles and cured at 80 °C for 2 h. After curing, the PDMS was separated from the master SU8 mold and placed in a reactive ion etcher (CS1701F RIE) for oxygen plasma treatment at 40 W of power for 30 s. The oxygen plasma treatment generates a hydrophilic surface on PDMS enables it to bond to the glass substrate. As the final step in device fabrication, the top electrode, bottom electrode and PDMS were aligned and bonded together. The total distance between bottom and top electrodes was 100 μm and the width of the inlet/outlet micro-channels was 200 μm . As shown in Fig. 1(b), cells were introduced to the device via the inlet port and are delivered to the microfluidic cavity containing the microwells situated between the top and the bottom electrodes. Cells were trapped inside microwells by the DEP and then lysis was performed using on chip electrodes. The chip was connected to a function generator (Tektronix AFG3021B) to carry out the DEP process and then to conduct cell lysis. An LCR meter is connected across the bottom and top electrodes to measure the impedance before and after trapping, and before and after lysis for full electronic characterization. Fig. 1(c) shows the photo of the completed microfluidic device (6.5 cm \times 4.5 cm).

3.2. Sample preparation

To demonstrate the functionality of the proposed single chip platform, human red blood cells used for trapping and lysis were extracted from human (female) whole blood samples mixed with

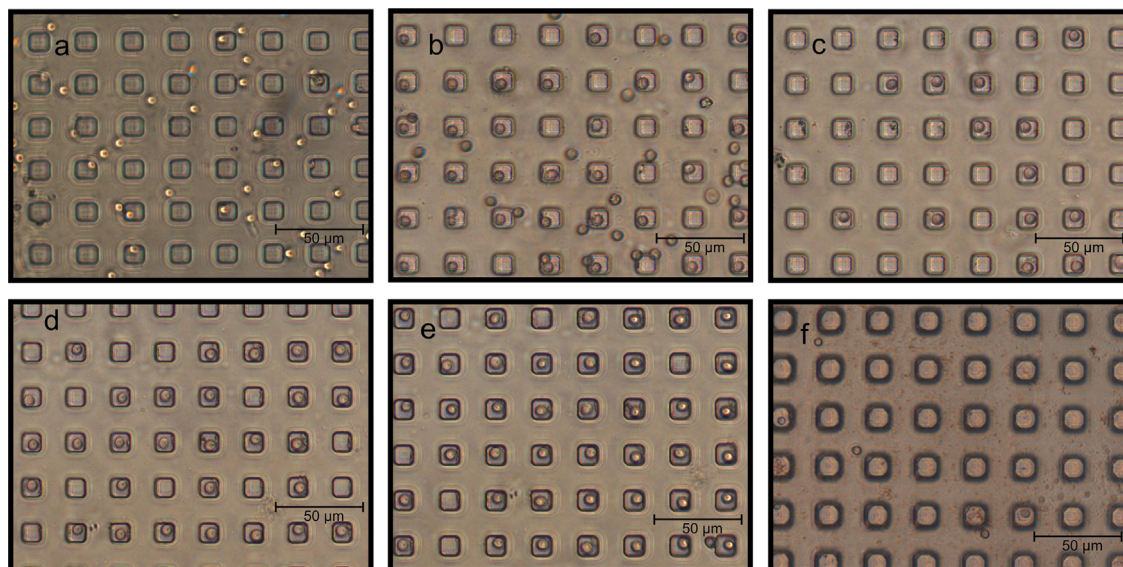


Fig. 2. Optical microscopy images of microwell arrays after introducing the cells into the microfluidic channel. (a) Before DEP; (b) after DEP, before washing; (c) 30% of wells are filled; (d) 60% of wells are filled; (e) 90% of wells are filled; (f) microwells after cell lysis.

EDTA (from Bioreclamation LCC, NY, USA). First, whole blood was centrifuged for 2 min at 1500 RPM to separate red blood cells. Subsequently, cells were washed twice to remove excess plasma. Phosphate-buffered saline (PBS) (calcium chloride, CaCl_2 , 1 g L^{-1} , magnesium chloride, $\text{MgCl}_2 \cdot 6\text{H}_2\text{O}$, 1 g L^{-1} , potassium chloride, KCl , 2 g L^{-1} , potassium phosphate monobasic, KH_2PO_4 , 2 g L^{-1} , sodium chloride, NaCl , 80 g L^{-1} , sodium phosphate dibasic, $\text{Na}_2\text{HPO}_4 \cdot 7\text{H}_2\text{O}$, 21.6 g L^{-1} , water) (Dulbecco and Vogt, 1954) was used as an isotonic solution for washing cells.

4. Results and discussion

4.1. Experimental and simulation results

Human red blood cells with a final concentration of $10^7 \text{ cells mL}^{-1}$ were introduced into the microfluidic device with $20 \mu\text{L min}^{-1}$ flow rate. The conductivity of the external medium was 0.01 S m^{-1} . To immobilize the cells using DEP, AC voltage of 80 kHz with 1.5 V amplitude was applied between the top and bottom electrodes. The non-uniform electric field distribution between the top and bottom electrodes caused the cells to experience positive dielectrophoresis at 80 kHz frequency (Sano et al., 2011; Hwang et al., 2008). Once a desired percentage of cells were trapped, the untrapped cells are washed with a continuous flow of PBS solution. As a first experiment we applied AC voltage for 23 s and observed that $30 \pm 2\%$ of wells remained filled with cells after a PBS wash. Subsequently the

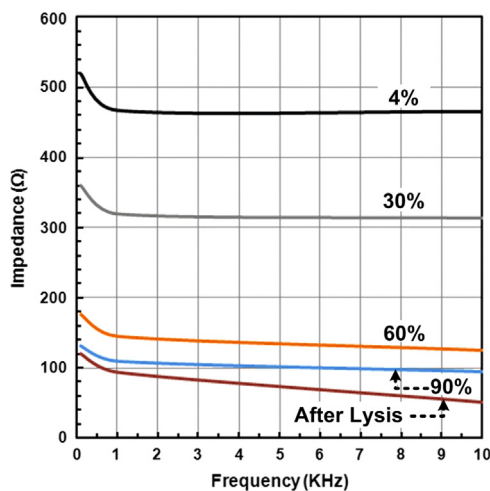


Fig. 3. A plot of impedance measurements versus frequency for different percentages of filled wells and after lysis.

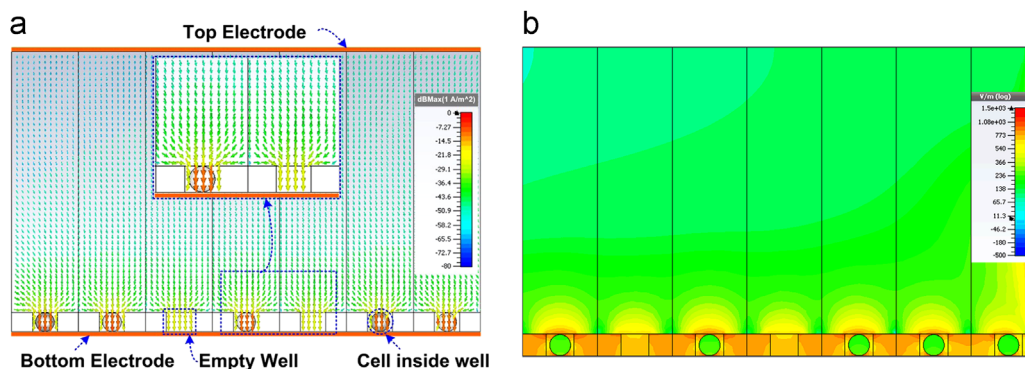


Fig. 4. (a) Simulated electric current distribution and (b) electric field distribution at 1 kHz frequency. Simulation was performed considering the presence of PBS in microwells and the cavity. Wells occupied by cells resulted in increase in current density increase compared to empty microwells.

impedance was measured at 100 Hz, 1 kHz and 10 kHz using an LCR meter. We observed that the application of AC voltage for 54 and 100 s resulted in $60 \pm 2\%$ and $90 \pm 2\%$ of the wells being filled with cells respectively. To induce lysis of the trapped cells, 2 V DC voltage was applied for 6 s between the top and bottom electrodes and the impedance was monitored at every step before lysis and after it. The optical images of micro-wells after introducing cells to the microfluidic device are shown in Fig. 2. Fig. 2(a) shows the device after introducing cells and before the application of the AC voltage. It shows that even before the application of DEP force some cells were already settled in the microwells as a result of gravity. To understand the contribution of gravitational force, the setup was maintained for 10 min before applying the DEP bias.

The untrapped cells were washed by flowing PBS through the channel. About 4% of the microwells were filled with cells due to gravity. Fig. 2(b) shows the wells after the DEP capture process, indicating that cells were dispersed both inside and outside the microwells. After this step, the voltage was turned off and cells outside the wells are washed and removed using the PBS solution rinse, before the impedance measurement. Fig. 2(c) shows the wells after removing the untrapped cells. In the first step, after applying AC electric field, 30% of the wells were filled with cells. Each well contained a single cell since the size of the wells closely matched the size of cells. Fig. 2(d) and (e) shows the image of the wells when 60% and 90% of the wells were filled with cells by applying AC electric field. The results of impedance measurement from wells that were about 4%, 30%, 60%, and 90% occupied with cells at 100 Hz, 1 kHz and 10 kHz are shown in Fig. 3. The impedance values decreased considerably as the fraction of filled micro-wells increased. To investigate changes in impedance due to presence of cells inside wells, the electric field and AC current distribution were simulated using electromagnetic wave simulation software (CST 2011 microwave studio) at 1 kHz. In this simulation, cavity and some wells were considered filled with cells and others filled with PBS solution. The red blood cells were considered as a multi-shell particle consisting of two shells, with $6.992 \mu\text{m}$ inner shell diameter and $7 \mu\text{m}$ outer shell diameter. The distance between the top and bottom electrodes was set to $100 \mu\text{m}$. Simulated electric current is shown in Fig. 4(a). As seen in Fig. 4(a), when wells were filled with cells the current density was found to increase in the microwells. Increasing current density translates into reduced impedance between the top and bottom electrodes, which is in agreement with experimental observations. Fig. 4(b) shows the electric field simulation result. It shows that electric field at the edge of wells are higher which results in trapping of the cells inside of wells.

After the DEP process, the trapped cells were lysed by the application of 2 V DC voltage between the top and bottom electrodes for 10 s. Fig. 2(f) shows the optical image of the wells

after cell lysis. After the application of DC voltage, $87 \pm 3\%$ of the cells were lysed. Red blood cell membrane has about -10 mV potential at the rest condition. When an external electric field is applied to the cells it induces additional potential in the cell membrane which makes it permeable to the external medium. This permeability is dependent on the strength and duration of the applied electric field. With the increase in electric field, cell membrane becomes more permeable to the external medium causing cell lysis. After lysis, the impedance was measured between the electrodes and recorded. As indicated in Fig. 3, the measured impedance was significantly decreased after lysis of trapped cells. This decrease ranged between $\sim 20\%$ for 100 Hz to 1 kHz frequency and $\sim 5\%$ for 1–10 kHz. The reason for this

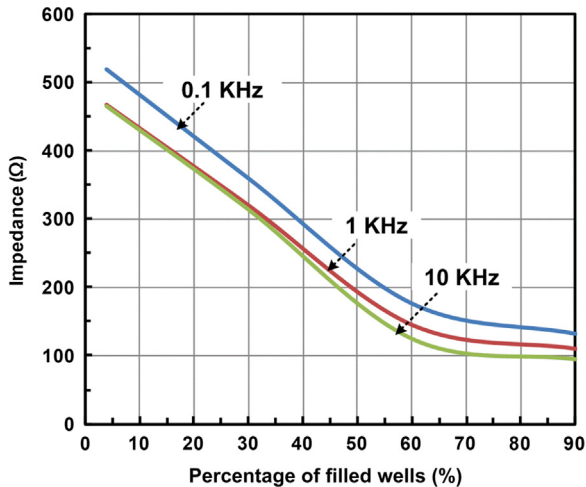


Fig. 5. Plot of measured impedance versus percentage of filled microwells for three different frequencies.

variation is that the cell and medium electrical parameters (conductivity and permittivity) are frequency dependent (Abdalla, 2011; Yoon, 2011). Fig. 5 shows the impedance values before lysis versus the percentage of filled wells at three different frequencies, 0.1, 1 and 10 kHz. The impedance values decreased greatly ($\sim 5.5 \Omega/\%$) for 4–60% of filled wells, however it varied slowly ($< 0.67 \Omega/\%$ of filled well) for 60–90% of filled wells.

4.2. Equivalent electrical model

To understand the behavior of the impedance change with respect to percentage of filled wells, an equivalent electrical circuit model was developed (Fig. 6). In this model, a single cell is modeled as a double layer sphere with cell membrane capacitance (C_m) and resistance (R_m) in parallel, and the internal cell media (cytoplasm) resistance (R_i) in series (Yoon, 2011; Kwong et al., 2005; Baskurt et al., 2010). A single microwell filled with PBS is modeled as capacitance (C_w) and resistance (R_w) in parallel. Similarly, microfluidic cavity above the microwell array which is filled with a PBS solution is modeled with parallel capacitance (C_c) and resistance (R_c). The electrode–PBS interface is modeled using the double layer capacitance (C_{p1} , C_{p2}). The red blood cell electrical parameters including cell membrane resistivity and capacitance, internal conductivity of the cells for calculating the values of components in the model are extracted from published articles (Yoon, 2011; Hoffman et al., 1980; Mirtaheeri et al., 2005; Robertson, 1981; Gimsa et al., 1994; Jason E. Gordon et al., 2007). The electrode polarization capacitance is dependent on the electrode and electrolyte materials (Padmaraj et al., 2011). The presented table in Fig. 6(c) shows the final values for the equivalent circuit model. These values are fitted to the model to closely match the experimental data. The impedance variation of the circuit model exhibits a similar trend as in the experimental data. In both model and measurement, as the percentage of filled

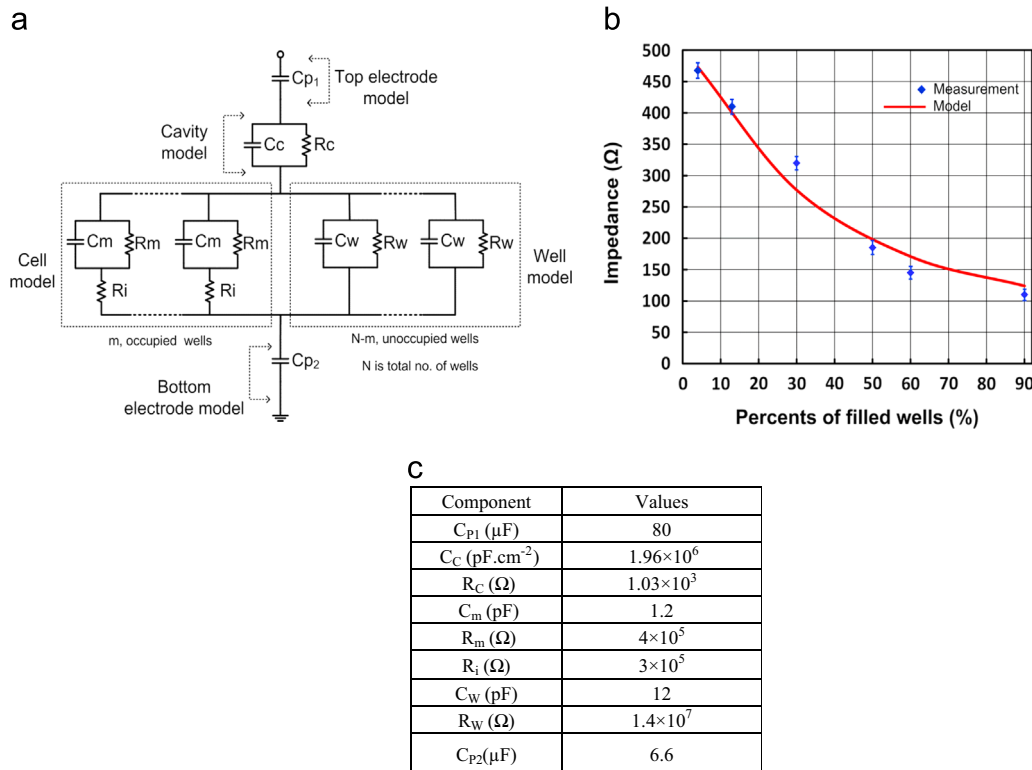


Fig. 6. (a) Equivalent electrical circuit model of the platform. The cells are modeled as the spherical double-shell particles with the capacitance of C_m (membrane capacitance). (b) Comparison of impedance for experiment and model at 1 kHz indicating close match. (c) Values of the circuit components used in the model at frequency of 1 kHz.

wells increases, the impedance decreases. The rate of change of impedance reduces for the case of greater than 60% of filled wells. There are some differences between the model and experimental results mostly at higher percentage of filled wells due to the limitation on defining the exact values for some parameters such as dielectric constant of the materials, cell membrane capacitances or cell conductivity. In addition, the dimension of the cells varies in practices which give rise to observed deviations. In practical applications this model can be used to extract the number of filled wells directly after DEP, from measured impedance, eliminating the need for optical monitoring. While this value may deviate from the actual number of cells, it is sufficient where the goal is to maximize trapping (evident by an observed decrease in impedance) before final cell lysis. The impedance measurement could direct the controller to increase the strength or the time of the dielectrophoretic AC field in order to increase the percentage of filled microwells with trapped cells. Once a maximum is reached as will be evident by a minimum in AC impedance, a DC electric field will be used to perform lysis as mentioned. Monitoring lysis using impedance measurement is quite straightforward. Impedance values following lysis are significantly lower ($5\times$) when 90% of the wells are filled (Fig. 3). Thus, the proposed lab-on-chip is ideal for trapping cells, and extraction of cellular materials using lysis, all using electric fields that can be realized in a compact manner. Moreover, impedance monitoring provides an effective substitute for optical monitoring of cell trapping and lysis. A single AA battery can supply the operational voltage and power requirement of the system. This enables a truly compact and portable solution for diverse applications in medical diagnostics where cell trapping and lysis are essential. Since a common electrode is shared between all the microwells in an array, the measured impedance is for the entire device. In future, one could re-engineer this platform where impedance measurement can be performed in each micro-well by patterning individually addressable electrodes per microwell. This will help one to work with mixture of cells and identify trapped cells in each microwell based on their impedance. Such an individually addressable microwell array can be used for trapping and identification of individual cells; it can also allow sorting and manipulation of individual cells based on non-optical impedance measurement in each microwell.

5. Conclusions

The paper details a non-optical fully-electronic approach for high throughput trapping of cells using AC dielectrophoresis, their lysis using a DC electric field and complete real-time monitoring of both processes using impedance spectroscopy. Equivalent circuit model correlates accurately with the impedance measurement that can be used to estimate the percentage of cells in the chip and to monitor lysis. Since this approach is an all-electronic monitoring and it does not require any optical components for monitoring it can be used in a truly compact lab-on-a-chip platform with potential applications in medical diagnostics where cell trapping and lysis are essential.

Acknowledgments

Authors would like to acknowledge the support of National Science Foundation through Grants NSF ECCS-0955024 and DBI-1063199, NSF Emerging Frontiers in Research and Innovation, Grant no.: 12404443 and the Tufts Collaborates! Initiative.

References

- Abdalla, S., 2011. *J. Mol. Liq.* 160, 130–135.
- Baek, S.K., Min, J., Park, J.H., 2010. *Lab Chip* 10, 909–917.
- Baskurt, O.K., Uyuklu, M., Meiselman, H.J., 2010. *IEEE Trans. Bio-med. Eng.* 57, 969–978.
- Bocchi, M., Lombardini, M., Faenza, A., Rambelli, L., Giulianelli, L., Pecorari, N., Guerrieri, R., 2009. *Biosens. Bioelectron.* 24, 1177–1183.
- Cha, M.S., Yoo, J., Lee, J., 2011. *Electrochem. Commun.* 13, 600–604.
- Cheng, I.F., Froude, V.E., Zhu, Y.X., Chang, H.C., Chang, H.C., 2009. *Lab Chip* 9, 3193–3201.
- Chung, C., Waterfall, M., Pells, S., Menachery, A., Smith, S., Pethig, R., 2011. *J. Electr. Bioimpedance* 2, 64–71.
- Di Carlo, D., Jeong, K.H., Lee, L.P., 2003. *Lab Chip* 3, 287–291.
- Dulbecco, R., Vogt, M., 1954. *J. Exp. Med.* 99, 167–182.
- Evander, M., Johansson, L., Lilliehorn, T., Piskur, J., Lindvall, M., Johansson, S., Almqvist, M., Laurell, T., Nilsson, J., 2007. *Anal. Chem.* 79, 2984–2991.
- Fritzsche, F.S.O., Dusny, C., Frick, O., Schmid, A., 2012. *Annu. Rev. Chem. Biomol.* 3, 129–155.
- Gascoyne, P.R.C., Noshari, J., Anderson, T.J., Becker, F.F., 2009. *Electrophoresis* 30, 1388–1398.
- Gimsa, J., Schnelle, Th., Zechel, G., Glaser, R., 1994. *Biophys. J.* 66, 1244–1253.
- Gordon, J.E., Gagnon, Z., Chang, H.C., 2007. *Biomicrofluidics* 1, 044102–044105.
- Gordon, Jason E., Gagnon, Zachary, Chang, Hsueh-Chia, 2007. *Biomicrofluidics* 1, 044102.
- Guido, I., Xiong, C.Y., Jaeger, M.S., Duschl, C., 2012. *Microelectron. Eng.* 97, 379–382.
- Hoffman, J.H., Kaplan, J.H., Callahan, T.J., Freedman, J.C., 1980. *Ann. N. Y. Acad. Sci.* 341, 357–360.
- Hwang, H., Choi, Y.J., Choi, W., Jang, J., Park, J.K., 2008. *Electrophoresis* 29, 1203–1212.
- Jen, C.P., Amstislavskaya, T.G., Liu, Y.H., Hsiao, J.H., Chen, Y.H., 2012. *Sensors—Basel* 12, 6967–6977.
- Khoshramesh, K., Zhang, C., Nahavandi, S., Tovar-Lopez, F.J., Baratchi, S., Mitchell, A., Kalantar-Zadeh, K., 2010. *J. Appl. Phys.* 108, 034904–034908.
- Kim, S.H., Yamamoto, T., Fourmy, D., Fujii, T., 2011. *Small* 7, 3239–3247.
- Kwong, C.C., Li, N., Ho, C.M., 2005. *Proc. SPIE* 6003, 60030N–60031N.
- Marcy, Y., Ouverney, C., Bik, E.M., Losekann, T., Ivanova, N., Martin, H.G., Szeto, E., Platt, D., Hugenholz, P., Relman, D.A., Quake, S.R., 2007. *Natl. Acad. Sci. USA* 104, 11889–11894.
- Matthew, K.H.S., Bryan, T., Real, Maria E., Bashir, M.A., Fry, Paul W., Fischer, Peter, Im, Mi-Young, Schrefl, Thomas, Allwood, Dan A., Haycock, John W., 2010. *IEEE Magn. Lett.* 1, 1500104.
- Mirtaheeri, P., Grimnes, S., Martinsen, O.G., 2005. *IEEE Trans. Bio-med. Eng.* 52, 2093–2099.
- Morgan, T.S., Hywel, Holmes, David, Shady, Gawadand, Green, N.G., 2007. *J. Phys. D: Appl. Phys.* 40, 61–70.
- Padmaraj, D., Miller, J.H., Wosik, J., Zagodzdon-Wosik, W., 2011. *Biosens. Bioelectron.* 29, 13–17.
- Piersimoni, C., Gherardi, G., Nista, D., Bornigia, S., 2009. *J. Clin. Microbiol.* 47, 282–283.
- Pohl, H.A., 1951. *J. Appl. Phys.* 22, 869–871.
- Pommer, M.S., Zhang, Y., Keerthi, N., Chen, D., Thomson, J.A., Meinhart, C.D., Soh, H.T., 2008. *Electrophoresis* 29, 1213–1218.
- Robertson, J.D., 1981. *J. Cell Biol.* 91, 189–204.
- Sano, M.B., Caldwell, J.L., Davalos, R.V., 2011. *Biosens. Bioelectron.* 30, 13–20.
- Sedgwick, H., Caron, F., Monaghan, P.B., Kolch, W., Cooper, J.M., 2008. *J. R. Soc. Interface* 5, S123–S130.
- Sun, S.G., Tao, Bernabini, Catia, Green, Nicolas G., Morgan, Hywel, 2007. *Meas. Sci. Technol.* 18, 2859–2868.
- Valero, A., Merino, F., Wolbers, F., Lutge, R., Vermes, I., Andersson, H., van den Berg, A., 2005. *Lab Chip* 5, 49–55.
- Yoon, G., 2011. *World Acad. Sci. Eng. Technol.* 60, 640–643.
- Zhang, H., Liu, K.K., 2008. *J. R. Soc. Interface* 5, 671–690.